Journal of Hydroscience and Hydraulic Engineering
Vol. 11, No. 2, January, 1944, 57-67

NUMERICAL ANALYSIS OF TURBULENT OPEN-CHANNEL FLOW OVER A VEGETATION LAYER USING A k-ε TURBULENCE MODEL

By

Yoshihiko SHIMIZU
Research Associate, Department of Civil Engineering, Gunma University
1-5-1, Tenjin-cho, Kiryu, 376, Japan

and

Tetsuro TSUJIMOTO
Associate Professor, Department of Civil Engineering, Kanazawa University
2-40-20, Kodatsuno, Kanazawa, 920, Japan

ABSTRACT

Open channel flow over a vegetation layer is numerically analyzed with a k-ε turbulence model. In the vegetation layer, complicated geometry of vegetation elements are characterized by form drag spatially averaged in the calculation mesh. Such a drag effect is taken into account not only in the momentum equations but in k- and ε-equations. The present model requires two additional parameters which are determined so as to reproduce a few examples of turbulence measurements of quasi-uniform flow over vegetated beds in laboratories. Next, it is certificated that the numerical values of these parameters are universal by more data from turbulence measurements when the other parameters which also appear in the ordinary k-ε model are kept as standard values.

INTRODUCTION

The characteristics of turbulent flow over a vegetation layer is one of the most fundamental topics of hydraulics of flow with vegetation. The purpose of this study is to establish a method of calculation for open-channel flow over vegetation, including the turbulence characteristics (statistical properties), using the experimental data of turbulence measurements in the flumes made by the authors (9, 12). Previous studies were reviewed in our references (11, 12). The hydraulic resistance was studied empirically in 1960s, while recently the turbulent structure has been focused on.

Numerical models of turbulent flow using higher order closures have been developed, and various types of flow have been analyzed. In particular, a k-ε turbulence model has been widely applied in the field of hydraulics since the efforts of Rodi et al. (7).

In analyzing the flow within a vegetation layer, the actual boundary is spatially complicated. Moreover, in order to describe the boundary accurately, the flow over a vegetation layer cannot be treated as a two-dimensional flow. Thus, the governing equation is spatially averaged in such a porous medium and the effect of individual roughness elements is taken into account by an averaged local drag force (averaged in a calculation mesh). Such a technique was introduced in analyzing canopy flow in the field of meteorology by Wilson & Shaw (14), and some reseachers (3, 13) followed them.

In this paper, open-channel flow over a bed covered by a vegetation layer is numerically analyzed by locally averaged governing equations. The presence of individual vegetation elements is accounted for the spatially averaged drag force acting upon individual elements. A k-ε model of turbulence is employed, and the drag effect is considered not only in the momentum equation but also in k and ε equations. The calculated results are compared with turbulence measurements made in flumes (9, 12) in order to determine the numerical values of the parameters involved in the model, and to certificate the applicability of the model for flow over vegetation layers with different densities.

SPATIALLY AVERAGING PROCEDURE

In this chapter, the spatial averaging procedure is explained. When the spatially averaged velocity is represented by $<u_i>$, the instantaneous local velocity, $u_i(x,y,z)$, is written as

$$u_i(x,y,z,t) = <u_i(t)> + u_i''(x,y,z,t) \tag{1}$$

in which x,y,z=spatial coordinates; t=time; $u_i=(u,v,w)$, $u_i''(x,y,z,t)$=perturbation from the spatially averaged velocity. On the other hand, when the time-averaged velocity is expressed by $\overline{u_i}$,

$$u_i(x,y,z,t) = \overline{u_i}(x,y,z) + u_i'(x,y,z,t) \tag{2}$$

where $u_i'(x,y,z,t)$=perturbation from the time averaged velocity, or the turbulence measured by point measurement. Eq.2 is termed "Reynolds decomposition."

As the vertical two-dimensional flow is dealt with here, spatial averaging means averaging in the horizontal plane (x,z). Such a spatial averaging operator $<\bullet>$ is defined as

$$<\Psi> \equiv \frac{1}{A}\iint_R \Psi(x,z)\,dx\,dz \tag{3}$$

in which Ψ represents a physical quantity; A, R=area and boundary of domain for averaging. As for the above operator, the following manipulations are valid.

$$<\Psi+\Phi> = <\Psi>+<\Phi> \quad ; \quad <\Psi\times<\Phi>> = <\Psi>\times<\Phi> \tag{4}$$

However, the order of spatial derivation and spatial averaging cannot be always exchanged with each other, as follows:

$$<\frac{\partial \Psi}{\partial x_i}> \neq \frac{\partial <\Psi>}{\partial x_i} \tag{5}$$

The reason of the above is explained as follows: According to Green's theorem,

$$<\frac{\partial \Psi''}{\partial x_i}> \equiv \frac{1}{A}\iint_R \frac{\partial \Psi''}{\partial x}\,dx\,dz = \frac{1}{A}\left(\int_{C_0} \Psi''\,dz + \sum_j \int_{C_j} \Psi''\,dz\right) \tag{6}$$

where C_0=boundary of averaging domain; and C_j=boundary of individual roughness elements (see Fig.1). The first term of the right side of the above equation becomes zero when the integrating domain is large enough to achieve the spatial homogeneity, but the second term is not zero unless the integrated function is constant along each individual roughness element. Hence,

$$<\frac{\partial \Psi''}{\partial x_i}> \neq \frac{\partial <\Psi''>}{\partial x_i} = 0 \tag{7}$$

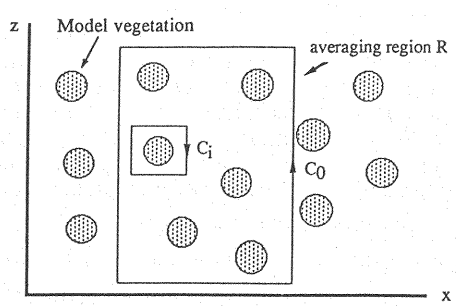

Fig.1 A horizontal averaging region within the vegetation

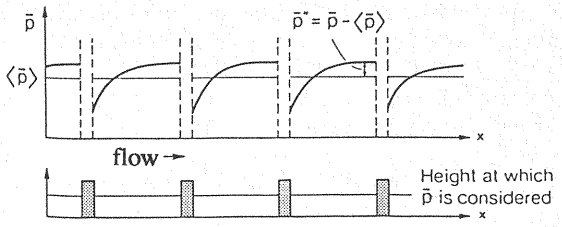

Fig.2 Schematic pressure field about a series of impermeable fence lying across the flow[6)]

As for the time averaged pressure, $\overline{p}$, in the flow field including roughness elements as shown in Fig.2 (quoted from Raupach & Shaw (6)), it is obvious that $\partial\overline{p}/\partial x=\partial\overline{p}''/\partial x>0$ and its horizontal average is never zero ($<\partial\overline{p}''/\partial x>\neq 0$); while obviously $\partial<\overline{p}''>/\partial x=0$. On the other hand, the velocity, u_i is zero along the boundary surface of the roughness elements, and the order of spatial derivation and spatial averaging can be exchanged each other. Then the continuity equation can be rewritten as follows.

$$\frac{\partial u_i}{\partial x_i}=\frac{\partial\overline{u_i}}{\partial x_i}=\frac{\partial u'_i}{\partial x_i}=\frac{\partial<u_i>}{\partial x_i}=\frac{\partial u''_i}{\partial x_i}=\frac{\partial\overline{u''_i}}{\partial x_i}=0 \tag{8}$$

GOVERNING EQUATIONS

The Reynolds equation where the viscous term is neglected is written as follows:

$$\frac{\partial U_i}{\partial t}+U_j\frac{\partial U_i}{\partial x_j}=-\frac{1}{\rho}\frac{\partial P}{\partial x_i}+\frac{\partial}{\partial x_j}(-\overline{u_iu_j}) \tag{9}$$

in which ρ=mass density of fluid, the capital letters represent the time average and the small letters the deviation from the time average. Next the each quantity is divided into the spatial average and the deviation from it as follows:

$$U_i=<U_i>+U_i'' \;;\qquad P=<P>+P'' \;;\qquad -\overline{u_iu_j}=<-\overline{u_iu_j}>+(-\overline{u_iu_j})'' \tag{10}$$

Substituting Eq.10 into Eq.9 and averaging the resultant equation in the horizontal plane, one obtaines the following equation.

$$\frac{\partial<U_i>}{\partial t}+<U_j>\frac{\partial<U_i>}{\partial x_j}=-\frac{1}{\rho}\frac{\partial<P>}{\partial x_i}-\frac{1}{\rho}\left<\frac{\partial P''}{\partial x_i}\right>+\frac{\partial}{\partial x_j}<-U_i''U_j''>+\frac{\partial}{\partial x_j}<-\overline{u_iu_j}> \tag{11}$$

where $<-U_i''U_j''>$ is the covariance of the spatial correlation of the time averaged components and termed the "dispersive flux" (6).

Multiplying the equation above by $<U_i>$, one obtains the spatially averaged energy transport equation of the mean flow energy, as follows:

$$\left(\frac{\partial}{\partial t}+<U_j>\frac{\partial}{\partial x_j}\right)\left(\frac{<U_i><U_i>}{2}\right)=-\frac{1}{\rho}\frac{\partial<P><U_i>}{\partial x_i}-\frac{1}{\rho}\left<\frac{\partial P''}{\partial x_i}\right><U_i>$$
$$-(<-U_iU_j>+<-\overline{u_iu_j}>)\frac{\partial}{\partial x_j}<U_i>+\frac{\partial}{\partial x_j}\left[\left(<-U_iU_j>+<-\overline{u_iu_j}>\right)<U_i>\right] \tag{12}$$

In the case of spatially averaged flow in the vegetation layer, $<\partial P''/\partial x_j>$ corresponds to the spatially average of drag force for each vegetation element, and thus,

$$\left<\frac{\partial P''}{\partial x_i}\right>=\frac{1}{2}\rho\lambda C_{di}<U_i>\sqrt{<U_j><U_j>} \tag{13}$$

where λ=vegetation density (projected area to the flow per unit volume of water); and C_{di}=drag coefficient in the i-th direction. This term expresses a sink of momentum in the mean flow, and the energy corresponding to this term is converted to tturbulent energy.

By introducing the kinematic eddy viscosity ν_t, the velocity gradient is related to the total of the spatially averaged Reynolds stress and the dispersive flux. Namely,

$$<-U_iU_j>+<-\overline{u_iu_j}> = \nu_t\left(\frac{\partial<U_i>}{\partial x_j}+\frac{\partial<U_j>}{\partial x_i}\right)-\frac{2}{3}<k>\delta_{ij} \tag{14}$$

where k=turbulent energy; and δ_{ij}=Kronecker's delta. The kinematic eddy viscosity is related to the turbulent energy k and the turbulent dissipation rate ε by Launder & Spalding (2), as follows.

$$\nu_t = \frac{C_\mu<k>^2}{<\varepsilon>} \tag{15}$$

in which C_μ=empirical parameter.

Although the transport equations of $<k>$ and $<\varepsilon>$ must be deduced by spatially averaging the ordinary k- and ε-equations of the standard k-ε model, the additional terms to them due to the drag effect are here assumed as follows.

$$\left<\frac{\partial P''}{\partial x_i}\right><U_i> = \frac{1}{2}\rho\lambda C_{di}<U_i>^2\sqrt{<U_j><U_j>} \tag{16}$$

This is based on the consideration that the turbulent energy is additionally brought from the energy corresponding to Eq.16, and it increases the dissipation rate.

The spatially averaged governing equations (in the calculation mesh) for vertically two dimensional flow are written as follows, where < > is abbreviated.

$$U\frac{\partial U}{\partial x}+V\frac{\partial U}{\partial y} = g\sin\theta-\frac{\partial}{\partial x}\left(\frac{P}{\rho}\right)-F_x+\frac{\partial}{\partial x}\left(2\Gamma\frac{\partial U}{\partial x}\right)+\frac{\partial}{\partial y}\left[\Gamma\left(\frac{\partial U}{\partial y}+\frac{\partial V}{\partial x}\right)\right] \tag{17}$$

$$U\frac{\partial V}{\partial x}+V\frac{\partial V}{\partial y} = -g\cos\theta-\frac{\partial}{\partial y}\left(\frac{P}{\rho}\right)-F_y+\frac{\partial}{\partial x}\left[\Gamma\left(\frac{\partial U}{\partial y}+\frac{\partial V}{\partial x}\right)\right]+\frac{\partial}{\partial y}\left(2\Gamma\frac{\partial V}{\partial y}\right) \tag{18}$$

$$U\frac{\partial k}{\partial x}+V\frac{\partial k}{\partial y} = \frac{\partial}{\partial x}\left[\left(\frac{\nu_t}{\sigma_k}+\nu\right)\frac{\partial k}{\partial x}\right]+\frac{\partial}{\partial y}\left[\left(\frac{\nu_t}{\sigma_k}+\nu\right)\frac{\partial k}{\partial y}\right]+P_k-\varepsilon+C_{fk}(F_xU+F_yV) \tag{19}$$

$$U\frac{\partial \varepsilon}{\partial x}+V\frac{\partial \varepsilon}{\partial y} = \frac{\partial}{\partial x}\left[\left(\frac{\nu_t}{\sigma_k}+\nu\right)\frac{\partial \varepsilon}{\partial x}\right]+\frac{\partial}{\partial y}\left[\left(\frac{\nu_t}{\sigma_k}+\nu\right)\frac{\partial \varepsilon}{\partial y}\right] +\frac{\varepsilon}{k}\left\{C_1[P_k+C_{f\varepsilon}(F_xU+F_yV)]-C_2\varepsilon\right\} \tag{20}$$

$$P_k = \nu_t\left\{2\left[\left(\frac{\partial U}{\partial x}\right)^2+\left(\frac{\partial V}{\partial y}\right)^2\right]+\left(\frac{\partial U}{\partial y}+\frac{\partial V}{\partial x}\right)^2\right] \tag{21}$$

$$F_x = \frac{1}{2}\rho\lambda C_{dx}U\sqrt{U^2+V^2}\ ; \qquad F_y = \frac{1}{2}\rho\lambda C_{dy}U\sqrt{U^2+V^2} \tag{22}$$

where P_k=production of turbulent energy; $\Gamma\equiv\nu_t+\nu$; ν_t=eddy viscosity; g=gravitational acceleration; θ=bed slope; C_1, C_2, σ_k, σ_ε, C_{fk}, $C_{f\varepsilon}$=numerical parameters of the model. Except C_{fk} and $C_{f\varepsilon}$, standard values (7) were adopted as follows: C_1=1.44, C_2=1.92, C_μ=0.09, σ_k=1.0 and σ_ε=1.3. The

additional parameters, C_{fk} and $C_{f\varepsilon}$, should be determined by turbulence measurements for flow over a egetation layer, and it should be checked whether or not the numerical values are universal.

PROCEDURE OF NUMERICAL CALULATION

The pressure P is to be expressed as a sum of the static pressure and the deviation from it (P''), as follows:

$$P = \rho g(h-y)+P'' \tag{23}$$

Substitution of Eq.23 into the governing equations, results in the following common form.

$$\frac{\partial}{\partial x}\left(\Phi U-\Gamma\frac{\partial \Phi}{\partial x}\right)+\frac{\partial}{\partial y}\left(\Phi V-\Gamma\frac{\partial \Phi}{\partial y}\right)=S_{\Phi} \tag{24}$$

in which Φ=transported quantity (U, V, k , ε); and S_{Φ}=source term by the external force.

These equations were solved based on the TEACH-T code by Gosman & Ideriah (1). The governing equations were discretized on a staggered grid, and the SYMPLE algorithm by Patankar & Spalding (5) was employed. At the bottom boundary, the wall function was applied so that the mean velocity along the boundary at the lowest point of grid was given by the log law, and a local equilibrium condition ($P_k=\varepsilon$) was assumed at the lowest point to calculate k and ε there ($k=u_*^2\sqrt{C_\mu}$ and $\varepsilon=u_*^3/(\kappa y)$; u_*=shear velocity and κ=Kármán constant). At the free surface, an axial symmetric condition was applied at first, where the free surface was regarded as a central axis of duct flow, and then the equations were resolved by modifying the free-surafe boundary condition after Nezu-Nakagawa's methods (4). Longitudinally, cyclic boundary condition was employed to obtain a solution for uniform flow. The mesh employed for calculation was prepared as shown in Fig.3.

In calculation, the discharge and the depth are known conditions. The bottom shear stress can be obtained by extrapolation of Reynolds stress calculated in the free-surface region where it shows a triangular distribution. Then, the energy gradient is given by the estimated bottom shear stress.

After k is obtained, each component of turbulence intensity is calculated by using an algebraic stress relation proposed by Rodi (8), as follows:

$$\overline{u_i u_j} = k\left[\frac{2}{3}\delta_{ij}+\frac{(1-\gamma)\left(\frac{p_{ij}}{\varepsilon}-\frac{2}{3}\delta_{ij}\frac{P_k}{\varepsilon}\right)}{C_r+\frac{P_k}{\varepsilon}-1}\right] \tag{25}$$

in which γ=0.6; C_r=1.5; and p_{ij}=stress production. p_{ij} is defined as follows:

$$p_{ij} = -\overline{u_i u_k}\frac{\partial U_j}{\partial x_k}-\overline{u_j u_k}\frac{\partial U_i}{\partial x_k} \tag{26}$$

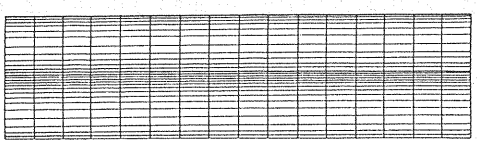

Fig.3 Mesh of numerical calculation (uniform flow)

COMPARISON WITH FLUME EXPERIMENTS

Flume experiments of flow over a vegetation layer were conducted in flumes (9,12), where the rigid (undeformable) cylinders of equal height (K) and diameter (D) were placed at equal spacings (s) in a square pattern on smooth flume beds (see Table 1). The drag coefficient was estimated as follows:

Table 1 Model vegetation in the flume experiments

Series	D (cm)	K (cm)	s (cm)	$\lambda \equiv D/s^2$ (cm^{-1})	equipped at
R	0.10	4.1	1.0	0.10	Kyoto University
A	0.15	4.6	2.0	0.0375	Kanazawa University

Table 2 Experimental conditions

RUN	H (cm)	h (cm)	I (10^{-3})	u_* (cm/s)	u_{*k} (cm/s)	U_m(cm/s)	h/K
R22	7.30	3.20	1.08	2.78	1.84	9.55	0.78
R24	9.48	5.38	1.00	3.05	2.30	12.78	1.31
R31	6.31	2.21	1.64	3.18	1.88	11.21	0.54
R32	7.47	3.37	2.13	3.95	2.65	13.87	0.82
R41	6.59	2.39	4.70	5.51	3.32	14.52	0.58
R42	7.35	3.25	2.63	4.35	2.89	17.16	0.79
R44	9.53	5.43	2.56	4.89	3.69	22.06	1.32
R53	8.41	4.30	4.35	5.98	4.28	23.31	1.05
R55	10.52	6.42	4.76	7.01	5.47	30.46	1.57
A11	9.50	4.91	1.06	3.14	2.26	13.25	1.07
A12	7.49	2.90	1.42	3.23	2.01	11.72	0.63
A31	9.36	4.77	2.60	4.88	3.48	19.59	1.04
A71	8.95	4.36	8.86	8.82	6.15	33.05	0.95

C_{dx}=1.0~1.5 and C_{dy}=0. A hot-film anemometer was used for turbulence measurements in Series R, while only the longitudinal velocity component was measured by a micro-propeller currentmeter (the diameter of the propeller was 3mm) in Series A. The turbulence measurements were conducted putting the probe of the instrument at the center of individual cylinders (apart $s/2$ from each cylinder).

In the experiments, uniform conditions were carefully kept by adjusting the weir at the downstream end of the flume. Table 2 shows the experimental conditions of runs refered to herein, where H=flow depth above the bottom; h=depth above the vegetation layer ($h \equiv H-K$); $u_* \equiv \sqrt{(\tau_0/\rho)}$; $u_{*k} \equiv \sqrt{\tau_k/\rho}$; $\tau_0 = \rho g H I$=bed shear stress; $\tau_k \equiv \rho g h I$; I=energy gradient; i_b=bed slope; and U_m=depth-averaged velocity.

In order to check the horizontal homogeneity of the flow field, measurements at several points (see Fig.4) in the same run were compared with each other. If the obtained velocity profiles are consistent with each other, then the numerical calculations based on the spatially averaged governing equations is reasonable to be compared with the data obtained by point measurements. These experiments treating homogeneous vegetation layer varying pattern of vegetation may bring about heterogenous flow, often with secondary currents.

Figure 5 shows the comparison of the mean velocity profile between measurements and calculated results. In order to obtain the best agreements between the measurement and calculation for Run R31, the additional parameters were determined: C_{fk}=0.07 and $C_{f\varepsilon}$=0.16. Then, the calculated results with the same values for the parameters were compared with the measured profiles. The figure demonstrates a good agreement between calculations and measurements through all the runs. The calculated Reynolds stress is compared with the measured data in Fig.6, and the present calculation well expressed the data.

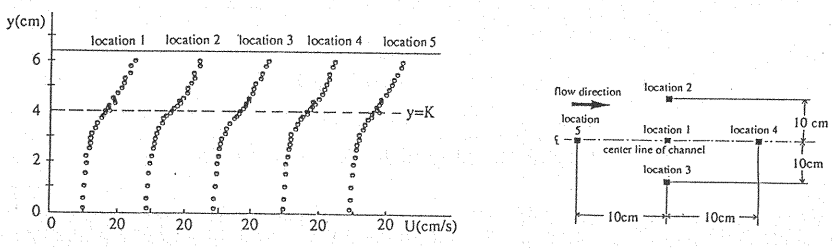

Fig.4 Velocity distribution at different locations relative to the vegetation elements

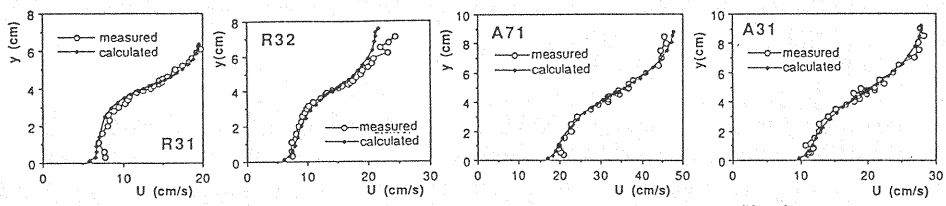

Fig.5 Velocity distribution of flow over vegetation-covered bed

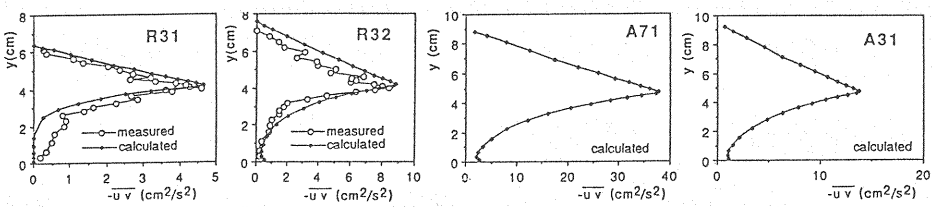

Fig.6 Reynolds-stress distribution over vegetation-covered bed

In the previous study (9, 12), it was found experimentally that the profiles of the velocity and the Reynolds stress in the vegetation layer followed exponential functions, as follows:

$$-\overline{uv} = -\overline{uv}\big|_{y=K}\exp[\alpha(y-K)] \qquad (y<K) \tag{27}$$

$$U(y)-U_s = (U_k-U_s)\exp[\beta(y-K)] \qquad (y<K) \tag{28}$$

in which α, β=empirical parameters; U_k=mean velocity at the vegetation boundary ($y=K$); and U_s=characteristic velocity in the vegetation layer ($\equiv\sqrt{2gI/(\lambda C_{dx})}$). The velocity profile deduced by a macroscopic force balance under the assumption of Eq.27 is well approximated by 28, and β is related to α (9, 12). However, one cannot obtain an equation to evaluate α except by experiments. The calculated profiles of Reynolds stress and velocity in the vegetation layer by the present model are consistent with Eqs.27 and 28, as shown in Figs.7 and 8.

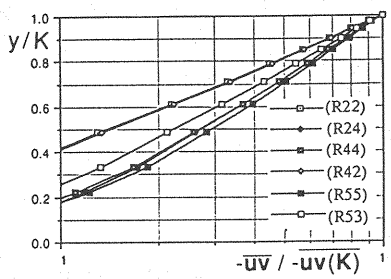

Fig.7 Reynolds-stress distribution in vegetation layer (calculation)

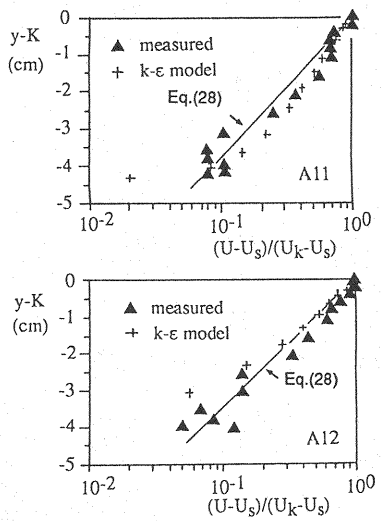

Fig.8 Velocity distribution in vegetation layer (calculation)

On the other hand, for the surface flow, the previous study (9, 12) proposed the folllowing velocity profile, which was deduced from mixing-length theory.

$$\frac{U(\eta)}{u_{*k}} = \frac{1}{\kappa}\ln\left[\frac{\kappa\eta}{l_0^*}+1\right] + \frac{U_k}{u_{*k}} = \frac{1}{\kappa}\ln\left[\frac{\eta+\delta}{\delta}\right] + \frac{U_k}{u_{*k}} \qquad (0<\eta<1) \qquad (29)$$

in which $\eta \equiv (y\text{-}K)/h$; $l_0^* \equiv l_0/h$; l_0=mixing length at the vegetation boundary; and $\delta \equiv l_0^*/\kappa$. δh may be termed the "shift of the theoretical wall" of the log-law. U_k and l_0 are fitting parameters which can be determined empirically. Shimizu et al.(9) deduced the relation among U_k and related l_0 with β and U_k. However, an estimation of α still remained. The calculated profile based on the present model is compared with Eq.29 in Fig.9. A good agreement is shown between them.

The parameter α was related to the parameter hI/K empirically in the previous study (9, 12), as follows:

$$\alpha\sqrt{sK} = -0.32\text{-}0.85\cdot\log\left(\frac{hI}{K}\right) \qquad (30)$$

The value of a determined from the result of the present numerical analyssis are plotted and compared with Eq.30 in Fig.10. As far as the range of the experiments, the present calculation suggests that Eq.30 is available, though wider applicability has to be checked by systematic inspection.

Figure 11 shows the turbulence intensity. The calculated results express the experimental data relatively well, though the former cannot express the convex profile of the latter in the vegetation layer.

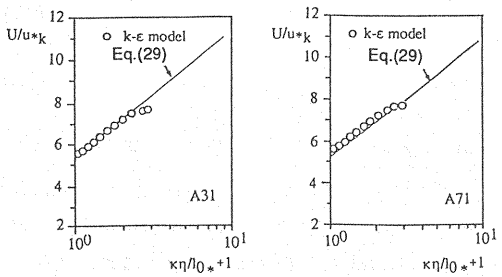

Fg.9 Free-surface flow velocity profile

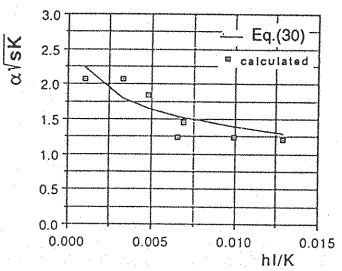

Fig.10 Relation between α and hI/K

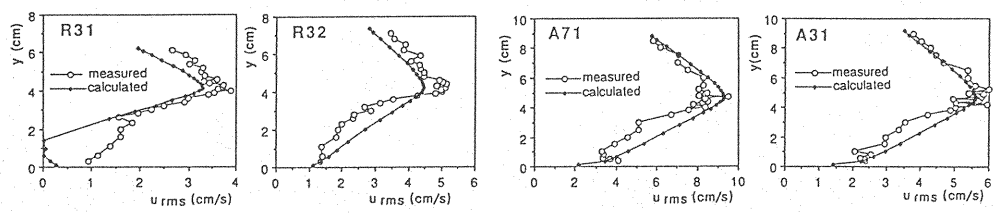

Fig.11 Distribution of turbulence intensity over vegetation-covered bed

APPLICATION TO UNESTABLISHED FLOW OVER A VEGETATED BED

The research was extended to unestablished flow over a vegetation layer. When the flow is introduced to the vegetated bed as shown in Fig.12, a transient process occurs where the turbulent characterstics change longitudinally to reach an equilibrium state sufficiently downstream. The numerical calculation was also conducted for the transient process, where the mesh as shown in Fig.13 was employed. At the upstream end of calculated region, fully established flow over a non-vegetated bed was assumed. In the calculation, discharge and depth were held constant. Actually, open-channel flow over the above mentioned bed never showed a linear free surface, but for simplicity the upper boundary of the mesh representing the free surface was assumed to be parallel to the x-axis. In the flume experiments, the water-surface was attempted to be held constant in the region x>0 by adjusting the weir at the downstream end of the flume. The vegetation model was the same to Series R for uniform flow experiments (9, 12). The experimental condition were set as H=8.31cm, I_e=0.00264, and U_m=18.44cm/s in the equilibrium reach.

The longitudinal change of the mean velocity profile is shown in Fig.14, where the measured data were plotted and the calculated profiles are drawn by dotted lines. The comparison between them demonstrates the applicability of the present model to non-uniform flow conditions. The comparison of the calculated Reynolds-stress distribution with the measured one is shown in Fig.15, and the present model can also explain the transient change of Reynolds-stress distribution.

In actual cases, the water-surface is not parallel to the bed. In such a case, the calculation mesh should be prepared in a curvilinear system corresponding to the water-surface profile estimated, for example, by a one-dimensional approach.

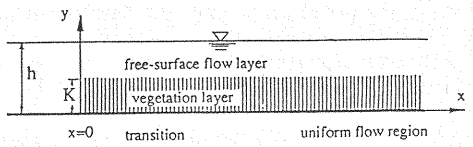

Fig.12 Schmatic figure of transition flow over vegetation-covered bed

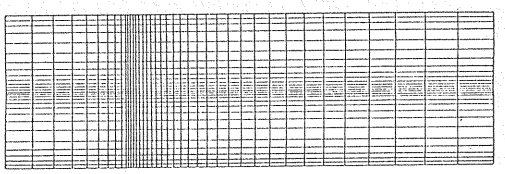

Fig.13 Mesh of numerical calculation (transition flow)

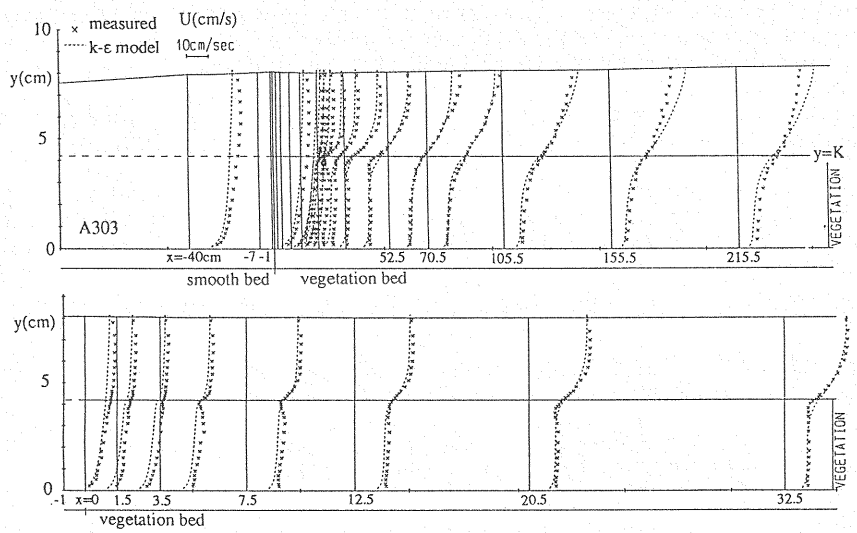

Fig.14 Longitudinal variation of velocity distribution

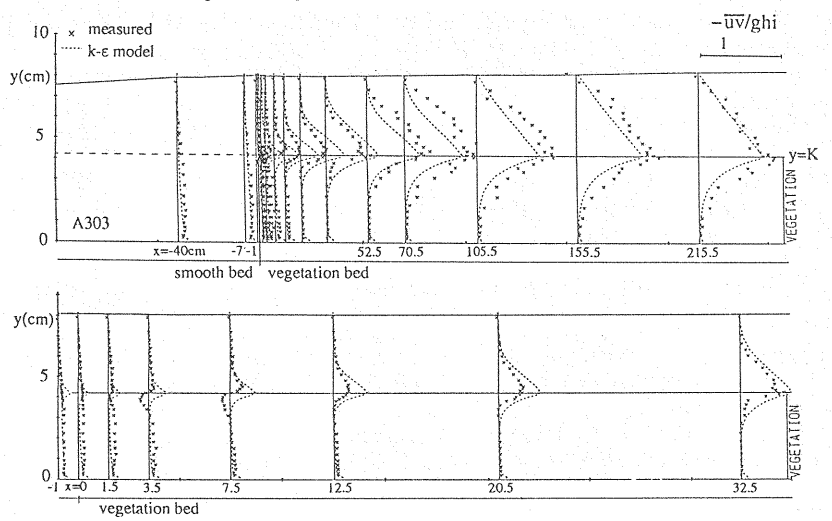

Fig.15 Longitudinal variation of Reynolds stress distribution

CONCLUSION

The results obtained in this paper are summarized below:

(1) The flow in a vegetation layer was analyzed numerically, and the governing equations were spatially averaged neglecting the geometry of individual vegetation elements. Then the modified governing equations were obtained by adding the terms due to the drag effect to the momentum, k and ε equations of the stardard k-ε model.

(2) By applying the technique of the TEACH-T code, the governing equations were numerically solved.

(3) The calculations based on the present model were executed for uniform flow conditions in an open-channel with vegetation, and the results were compared with the experimental data. Not only the velocity profile but also the statistical properties of turbulence can be described by the calculation based on the present model, where the specified model parameters can be rather universal, at least under the conditions of flow with idealized homogeneous vegetation.

(4) The calculated results are consistent with previous analysis, where an exponential distribution of the Reynolds stress induced in the vegetation layer was assumed, and the macroscopic force balance was considered in the vegetation layer, while a mixing length model was applied to the surface flow.

(5) The present model was applied to unestablished flow over a vegetation layer, which means the flow in the transient reach downstream of the beginning of the vegetated bed. The longitudinal changes of the profiles of velocity and Reynolds stress in the transient reach were calculated by assuming the water-surface elevation is paralle to the bed, and they showed good agreements with the measurements in the flume where the depth in the vegetated reach was tried to be kept as constant as possible.

The study suggets that the proposed numerical model is a good representation of flow over a vegetated bed. Since people are currently placing more environmental conditions, river engineering requires more knowledge about the characterstics of flow with vegetation. For example, such knowlege is needed to predict resistance, sediment transport, and bed deformation. The present model allows for calculations over vegetated bed to be made easily than by conducting physical experiments.

REFERENCES

1. Gosman, A.D. and J.K. Ideriah : *TEACH-T, A General Computer Program for Two-Dimensional Turbulent Recirculating Flows*, Dept. Mech. Engrg., Imperial College of Tech., London, S.W.7, 1976.
2. Launder, B.E. and D.B. Spalding : The numerical computation of turbulent flows, *Computer Methods in Applied Mech. & Engrg.*, Vol.3, pp.269-289, 1974.
3. Murakami, S., S. Kato, B.E. Launder, Y. Suzuki : Air flow characteristics of laminar-type clean room: Characteristics of diffusion of pollutant, *Seisan-Kenkyu*, Vol.40, No.1, pp.67-70, 1988 (in Japanese).
4. Nezu, I. and H. Nakagawa : Numerical calculation of open-channel flows by using a modified k-ε turbulence model, *Proc. JSCE*, No.387, pp.125-134, 1987 (in Japanese).
5. Patanker, S.V. and D.B. Spalding : A calculation procedure for heat, mass and momentum transfer in three-dimensional parabolic flows, *Int. Jour. Heat Mass Transfer*, ol.15, pp.1787-1806, 1972.
6. Raupach, M.R. and R.H. Shaw : Averaging procedures for flow within vegetation canopies, *Boundary Layer Meteorology*, Vol.22, pp.79-90, 1982.
7. Rodi, W. : *Turbulence Models and Their Applications*, IAHR Monograph, Delft, 1980.
8. Rodi, W. : A new algebraic relation for calculating the Reynolds stress, *ZAMM*, Vol.56, pp.219-221, 1976.
9. Shimizu, Y., T. Tsujimoto, H. Nakagawa and T. Kitamura : Experimental study on flow over rigid vegetation simulated by cylinders with equi-spacing, *Proc. JSCE*, No.438, pp.31-40, 1991 (in Japanese).
10. Shimizu, Y., T. Tsujimoto and H. Nakagawa : Numerical study on turbulent flow over rigid vegetation-covered bed in open channels, *Proc. JSCE*, No.447, pp.35-44, 1992 (in Japanese).
11. Tsujimoto, T. : Hydraulics of flow with vegetation in open channels, *Lecture Notes, 27th Summer Seminar on Hydraul. Engrg.*, Course A, JSCE, 91-A-5, pp.1-22, 1991 (in Japanese).
12. Tsujimoto, T., Y. Shimizu, T. Kitamura and T. Okada : Turbulent open-channel flow over bed covered by rigid vegetation, *Jour. Hydroscience & Hydraul. Engrg.*, JSCE, Vol.10, No.2, pp.13-26, 1992.

13. Uno, I., T. Ueda, S. Wakamatsu, A. Nakamura : A study on the formation mechanism of noctural urban boundary layer by turbulence closure model, *Proc. Environ. & Sanitary Engrg. Research,* JSCE, Vol.24, pp.125-136, 1988.
14. Wilson, N.R. and R.H. Shaw : A higher order closure model for canopy flow, *Jour. Applied Meteorology*, Vol.16, pp.1197-1205, 1977.

APPENDIX - NOTATION

The following symbols are used in this paper:

C_1, C_2, C_μ = numerical parameters of standard k-ε model;
C_{fk}, $C_{f\varepsilon}$ = additional numerical parameters due to drag effect;
C_{di} = drag coefficients of model-plants of the i-th direction;
D = diameter of model-plants;
g = gravity;
h = water depth above the vegetation (*H-K*);
H = depth (from bottom to surface);
I = energy gradient;
i_b = bed slope;
K = vegetation height;
l_0 = mixing length at y=K;
l^* $\equiv l/h$ = dimensionless mixing length;
s = distance between individual plants;
u_i = instantaneous velocity of the i-th direction;
U, V = mean velocity (time average);
U_k = velocity at the interface between vegetation and surface-flow region;
U_m = depth averaged velocity;
U_s =characteristic velocity in the vegetation layer
u_* $= \sqrt{gHI} = \sqrt{\tau_0/\rho}$ = shear velocity;
u_{*k} $= \sqrt{ghI} = \sqrt{\tau_k/\rho}$;
y = vertical distance from bed bottom;
α, β = reciprocals of length for velocity and Reynolds-stress profiles in vegetation layer;
γ = parameter of Rodi's algebraic stress model;
Γ = parameter of Rodi's algebraic stress model;
ν, ν_t = kinematic viscosity and kinematic eddy viscosity;
δ $\equiv l_0^*/\kappa$;
κ = Kármán constant;
λ $\equiv D/s^2$ = projected area of vegetation to the flow per unit volume of water;
σ_k, σ_ε = numerical parameters of standard k-ε model;
τ_0 = bed shear stress ($\equiv \rho gHI$);
τ_k = Reynolds stress at the top of vegetation;
Φ = physical quantity
η $\equiv y/h$; *and*
$< >$ = spatially averaged quantity.

(Received May 14, 1993; revised September 30, 1993)